Supporting information

3D-Printed Carbon Nanoparticle Monoliths Enabling Ultrahigh Mass Loading of NiCoAl Layered Double Hydroxides for Asymmetric Supercapacitors

*Jungeun Bae, Thang Cao Doan, Anisa Fitriani Rosyadi, Yebin Park, and Hyojong Yoo**

Department of Battery and Chemical Engineering, Hanyang University, Ansan, Gyeonggi-do, 15588, Republic of Korea

*Correspondence to: hjhaha73@hanyang.ac.kr

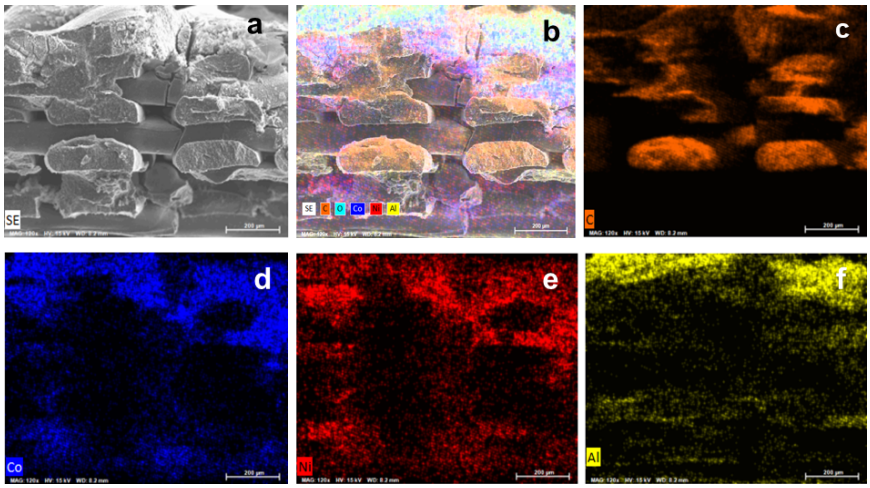

Figure S1: a) SEM image of cross-sectional NiCoAl-2-LDH@3D-PE; Elemental mapping for b) overall, c) C, d) Co, e) Ni, and f) Al.

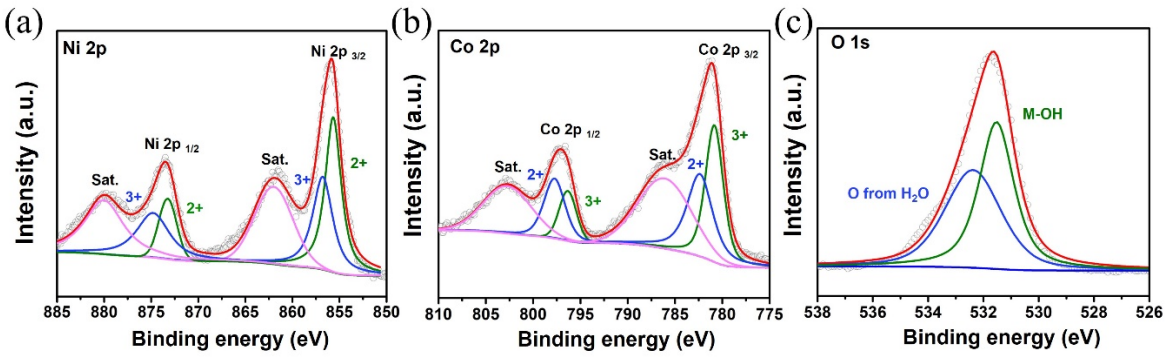

Fig. S2: The high-resolution XPS spectra of Ni 2p (a), Co 2p (b), and O 1s (c) for NiCo-LDH@3D-PE.

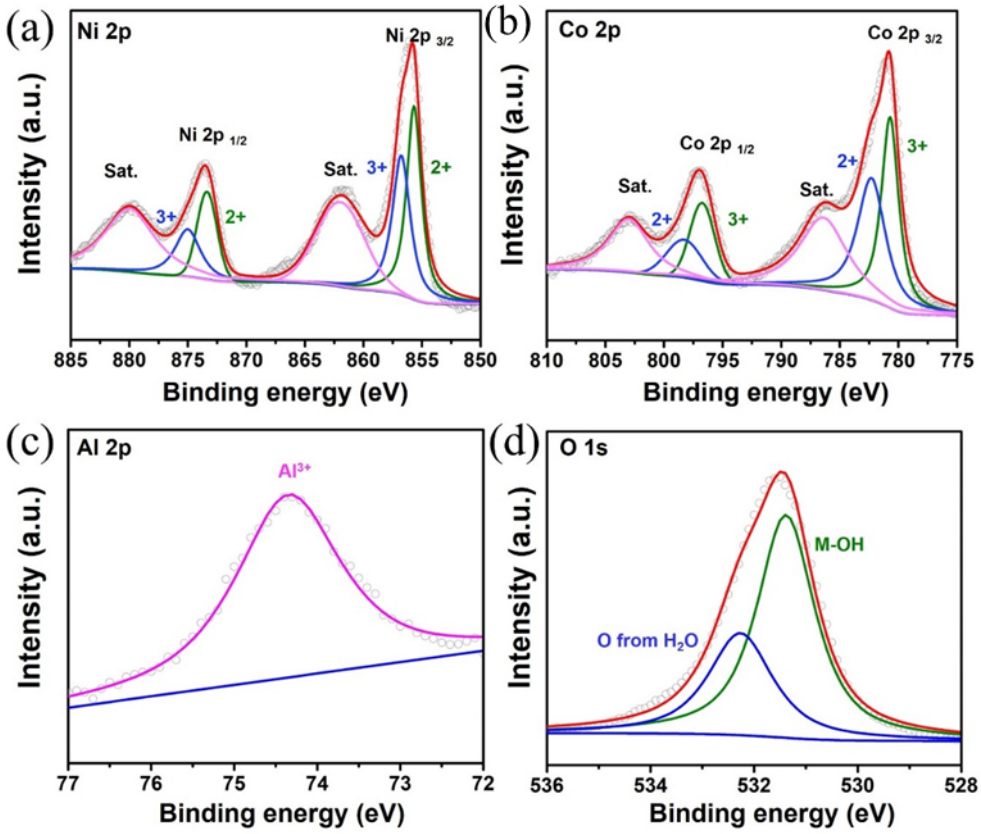

Fig. S3: The high-resolution XPS spectra of Ni 2p (a), Co 2p (b), Al 2p (c), and O 1s (d) for NiCoAl-LDH-5@3D-PE.

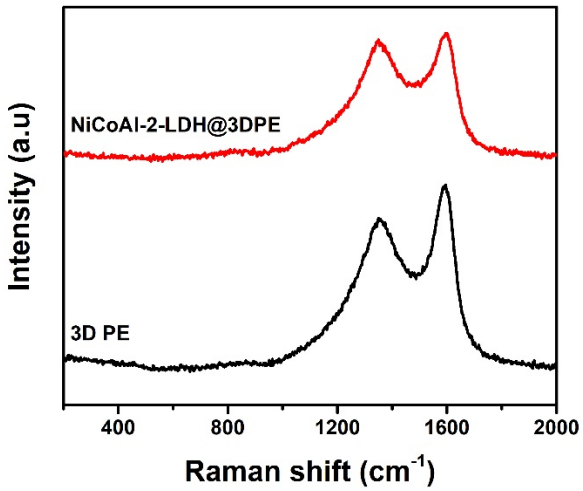

Fig. S4: Raman spectra of 3D-PE and NiCoAl-2-LDH@3D-PE

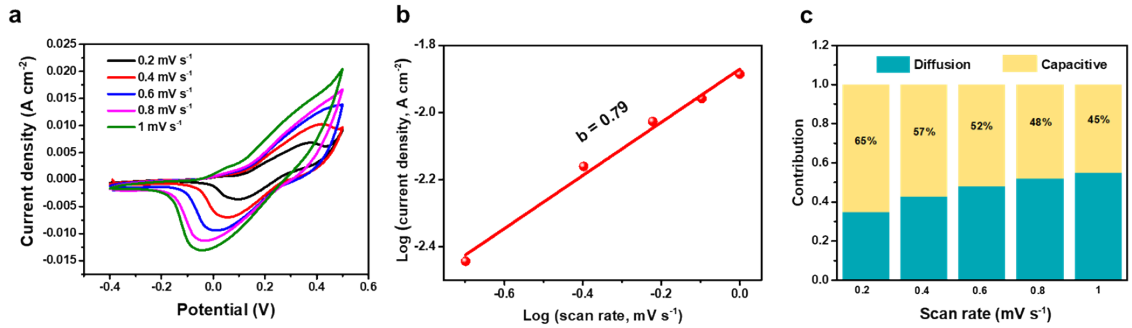

Fig. S5: a) CV curves response for NiCoAl-2-LDH@3D-PE at different scan rates. b) Calibration plot for log (υ/mV s^{-1}) vs. log (i_p/A cm^{-2}). c) Bar graph for contribution percentage between capacitive and diffusion-limited capacitances at different scan rates.

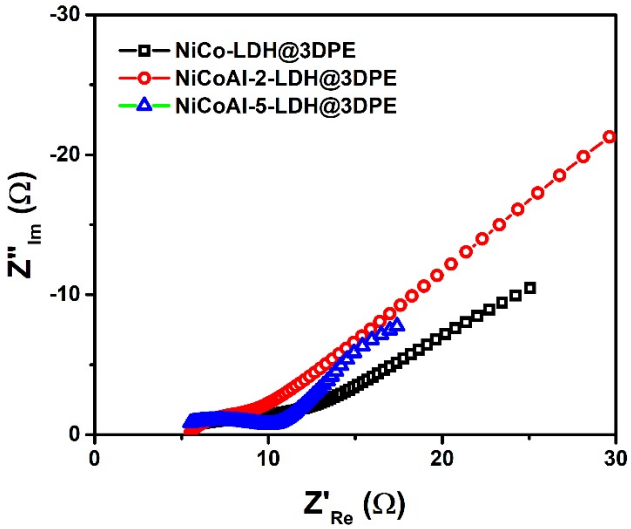

Fig. S6: Niquist plots of NiCo-LDH@3D-PE, NiCoAl-2-LDH@3D-PE, NiCoAl-5-LDH@3D-PE

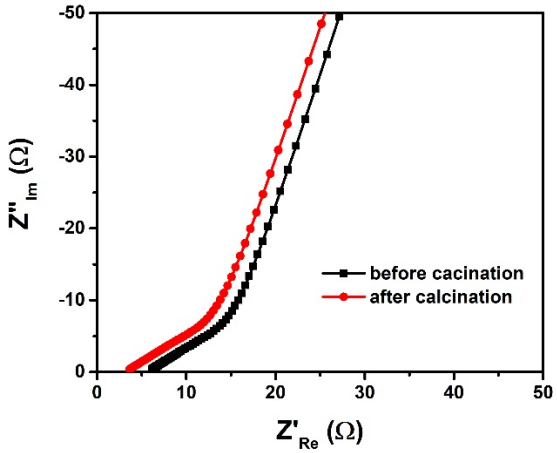

Fig. S7: Nyquist plot of 3D printed electrode before and after calcination.

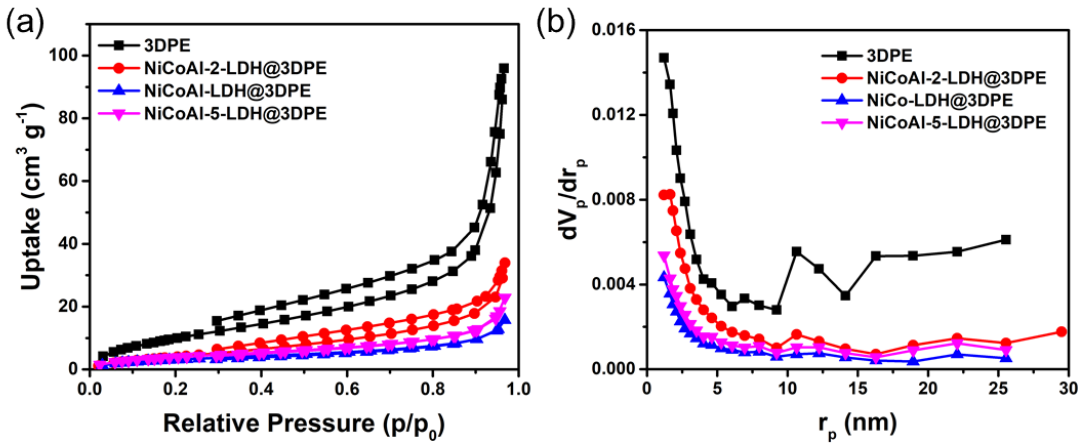

Fig. S8: a) N_2 adsorption isotherms and b) BJH curves of 3D-PE, NiCo-LDH@3D-PE, NiCoAl-2-LDH@3D-PE, and NiCoAl-5-LDH@3D-PE."

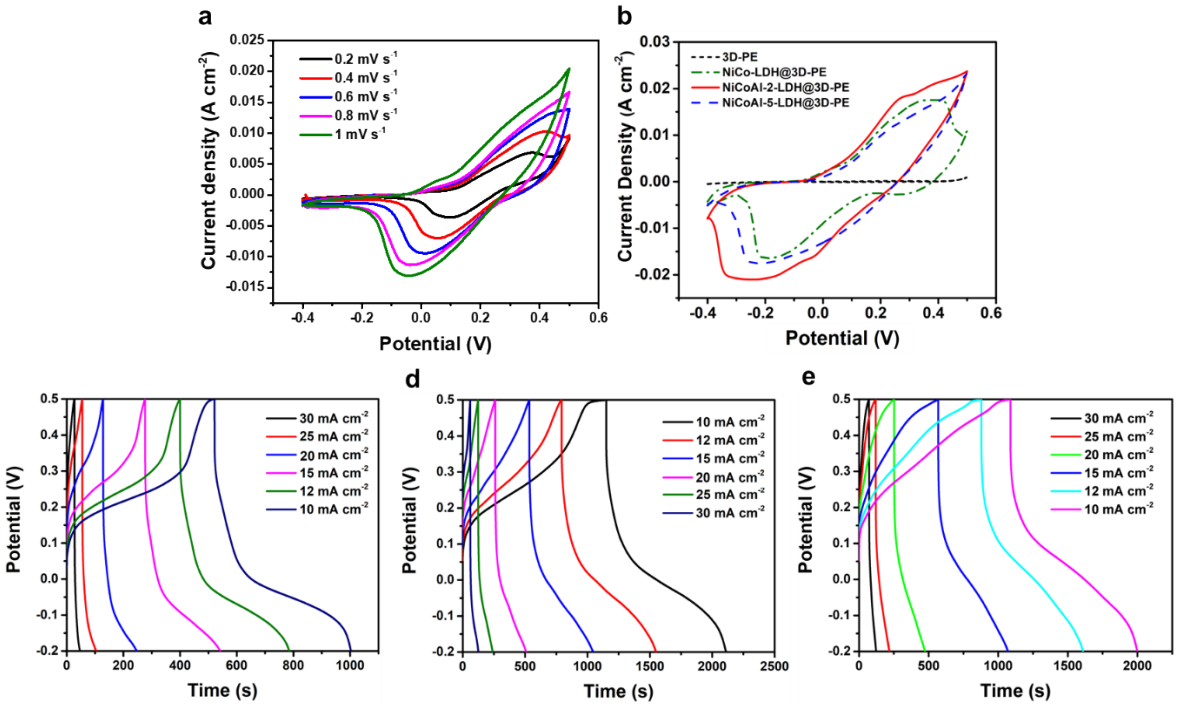

Fig. S9: a) CV curves of NiCoAl-2-LDH@3D-PE with different scan rate, b) CV curves of 3D-PE, NiCo-LDH@3D-PE, NiCoAl-2-LDH@3D-PE, and NiCoAl-5-LDH@3D-PE. GCD curves with different current density of c) NiCo-LDH@3D-PE, d) NiCoAl-2-LDH@3D-PE, e) NiCoAl-5-LDH@3D-PE.

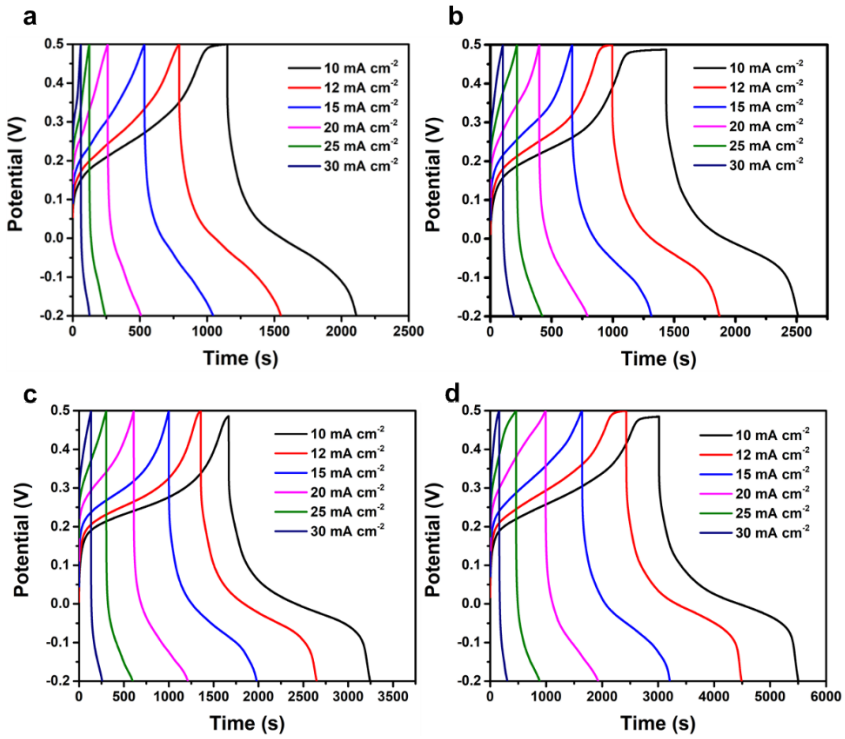

Fig. S10: GCD curves at different current densities of NiCoAl-2-LDH@3D-PE with the thickness of a) 0.8 mm, b) 1.6 mm, c) 2.4 mm, and d) 3.2 mm

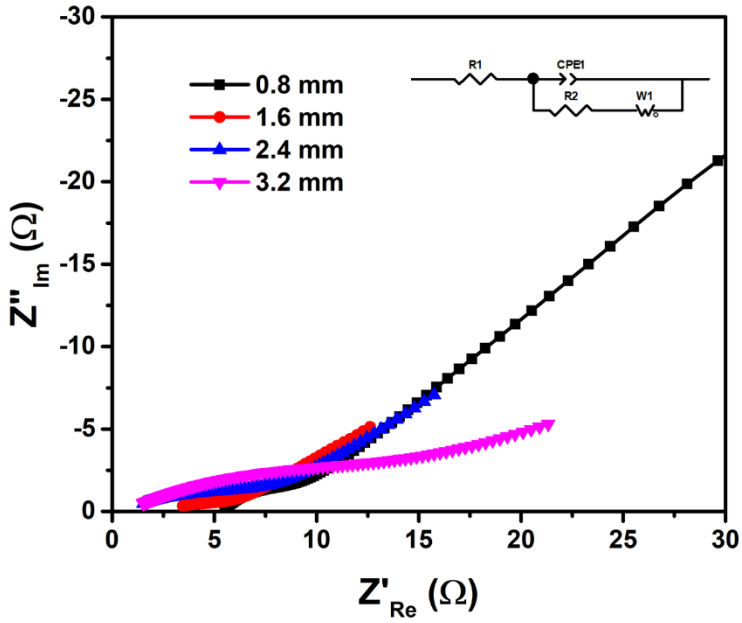

Fig. S11: Nyquist plots of NiCoAl-LDH-2@3D-PE with different electrode thickness

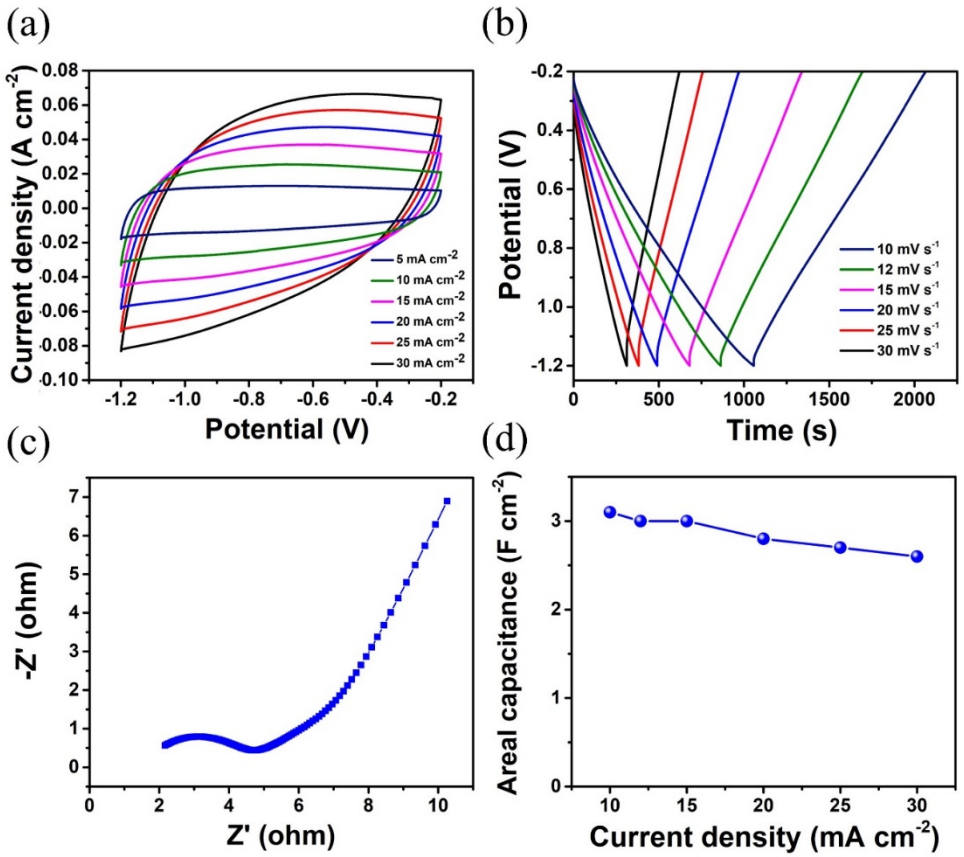

Fig. S12: Electrochemical performance of ATCC: (a, b) CV and GCD curves at different scan rate and different current densities. (c) Nyquist plot for ATCC. (d) Areal capacitance for different current densities.

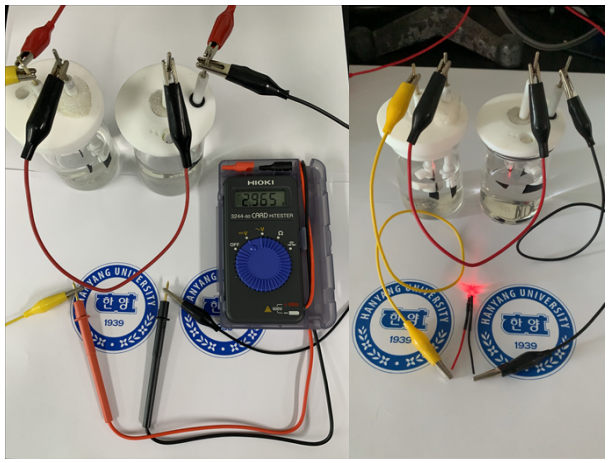

Fig. S13: digital images of 2 asymmetric supercapacitor devices NiCoAl-2-LDH@3D-PE//ATCC

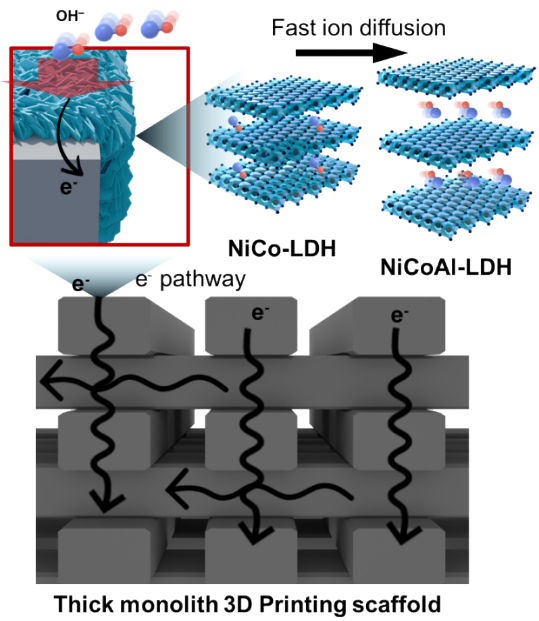

Fig. S14: schematic illustration of ion and electron transport pathways within the 3D-PE structure

Table S1: BET surface area, pore volume and mean pore diameter of 3D-PE and NiCoAl-2-LDH@3D-PE.

Samples	BET surface area (m^2 g^{-1})	Pore volume (cm^3 g^{-1})	Mean pore diameter (nm)
3D-PE	41.03	0.15	14.46
NiCo-LDH@3D-PE	12.46	0.02	7.80
NiCoAl-2-LDH@3D-PE	18.67	0.05	11.26
NiCoAl-5-LDH@3D-PE	15.48	0.04	9.12

Table S2: R_{esr} and R_{ct} of NiCoAl-LDH-2@3D-PE with different electrode thickness

Electrode thickness	R_{esr}	R_{ct}
0.8 mm	5.40	3.96
1.6 mm	2.37	5.06
2.4 mm	0.57	6.25
3.2 mm	0.56	8.74